

DROP WEIGHT IMPACT STRENGTHS OF POROUS CONCRETES INVESTIGATED WITH A MEASUREMENT TECHNIQUE USING LASER DOPPLER VELOCIMETRY

**AYDA S. AGAR OZBEK^{†*}, JAAP WEERHEIJM^{†^}, ERIK SCHLANGEN[†] AND KLAAS
VAN BREUGEL[†]**

[†] Delft University of Technology
Faculty of Civil Engineering and Geosciences, Delft, The Netherlands,
Email: aydasafakagar@gmail.com,
J.Weerheijm@tudelft.nl, H.E.J.G.Schlangen@tudelft.nl
K.vanBreugel@tudelft.nl, Web page: <http://www.tudelft.nl/>

^{*} Istanbul Technical University
Faculty of Civil Engineering, Istanbul, Turkey,
Email: sagar@itu.edu.tr, Web page: <http://www.itu.edu.tr/>

[^] TNO, Defence Security and Safety
Rijswijk, The Netherlands
Email: jaap.weerheijm@tno.nl, Web page: <http://www.tno.nl/>

Key words: Drop weight impact, Porous concrete, Laser, Impedance mismatch

Abstract: Porous concrete is used in many applications that require permeability, noise absorption or thermal insulation. However, its response under dynamic loading is generally not considered. Porous concrete has a characteristic of forming multiple cracks and subsequently fracturing into small fragments when exposed to impact loading. Therefore, with the aim of designing a special type of cementitious material for building protective structures, porous concrete was investigated. To be able to analyze the dynamic properties of the different types of porous concretes produced, an experimental configuration that reveals the dynamic response of porous concretes in a drop weight impact test was designed. Through the measurement of particle velocity at the interface between the impactor and the concrete target, the dynamic response was obtained. Laser Doppler velocimetry was used in monitoring the time history of the particle velocity at the interface which was subsequently analyzed using a special reverberation application of the impedance mismatch method. Measurements were conducted to demonstrate how the proposed experimental technique can be used on porous and normal concretes.

The consistency of the results from the experiments that were performed while testing the same porous concrete materials with different impactors are presented for the verification of the experimental configuration and the analysis method. The analyses of the particle velocity time histories of different porous concretes and a normal concrete are also demonstrated which showed that the measurement technique was sufficient to determine the impact strengths of different types of porous concretes as well as a normal concrete with a moderate strength. As the results are compared, it was observed that the aggregate properties and compaction, coupled to porosity, are the main factors that affect the impact strength of porous concrete.

1 INTRODUCTION

Porous concrete is a type of concrete incorporating a high amount of meso-size air voids that makes its physical characteristics markedly differ from normal concrete. Therefore, it is currently being used in various applications due to its enhanced permeability, noise absorption or thermal insulation [1-4]. A research project was undertaken to design a special type of porous concrete, that fractures into small fragments when exposed to impact loading while having sufficient static strength, to be used in protective structures such as safety walls or storages for explosives.

Although the key feature of the material that was aimed to be designed was its property of fracturing into small size fragments, quantifying the dynamic strengths of the different porous concrete mixtures was also essential to be able to better elaborate the dynamic properties of the material. This study presents the experimental configuration that has been developed in order to investigate the impact behaviour of porous concrete and the test results from various porous concretes that have been produced and investigated on the way to attaining the modified porous concrete that was aimed for.

The experimental configuration presented in this study is an easily applicable measurement technique that was developed to determine the particle velocity at the interface between the impactor and the target in a drop weight impact test. Apart from being easily applicable, the experimental configuration and the subsequent analysis technique have the advantage of involving the known dynamic impedance properties and the velocity measurements of only the impactor. Therefore, the target specimen that is being tested is not directly involved in the measurements or the analysis.

In planar impact experiments, there are various measurement techniques involved to quantify the velocity and pressure to be able to define the dynamic performance of a material [5]. Laser interferometry has become generally accepted as a competent tool for monitoring

the motion of the surfaces of shocked specimens [6-8]. Electromagnetic velocity gauges, piezo-resistive manganin stress gauges, accelerometers, Doppler-radar are only some of the other measurement equipment used in planar impact experiments [9-12]. In this work, Laser Doppler Velocimetry (LDV) is used as the monitoring technique. Laser Doppler velocimetry, also known as laser Doppler anemometry (LDA), is a non-contact diagnostic method, based on the Doppler principle, introduced by Yeh and Cummins [13]. A Doppler velocimeter system is capable of measuring the motion of a particle or surface which has a rapidly changing velocity. This property can, therefore, be employed to measure the motion of a free-falling projectile throughout an impact test to obtain the full velocity-time history. In research studies where LDV is used, the velocity signals captured are usually either differentiated to obtain the acceleration and multiplied by the impactor mass to attain the load-time relationship or used in energy calculations based on the change in kinetic energy [14-16]. In this study, LDV has been selected as the monitoring technique to acquire the velocity history data of the impact surface. The velocity measurements were then processed using the reverberation application of the impedance mismatch method to quantify the dynamic strengths of the concretes tested which will be presented in more detail in the Measurement and Analysis Techniques section.

2 EXPERIMENTAL INVESTIGATIONS

2.1 Materials

The summary of the compositional properties of the mixtures is given in Table 1. The cement used was CEM I 52.5 R. A set retarder that provides a workability time of up to 3 hours was also used. Crushed basalt and river gravel were sieved in size groups of 2-4 mm and 4-8 mm before use. Water to binder ratio was kept at 0.3 in all the mixtures. The preparation of the porous concretes was done

following a standardized procedure. During casting, two compaction techniques have been applied which were machine compaction using an impact hammer while the hammer was also rotated and hand compaction using a steel cylinder. Casting was done in layers of 2.5 cm. A moderate strength normal concrete was also produced and tested in order to verify whether

the experimental technique can be used for a moderate strength normal concrete or not.

Core samples of 60 mm diameter were then drilled from the specimens and cut at the fixed height of 70 mm to be tested at the drop weight impact test.

Table 1: Compositional properties of the porous concrete mixtures

Mixture code	PRC1	PRC2	PRC3	PRC4	PRC5	PRC6	PRC7	PRC8	PRC9
Aggregate composition									
Crushed basalt (2-4 mm) (gr)	-	-	-	2000	1000	-	-	2000	1000
Crushed basalt (4-8 mm) (gr)	2000	-	2000	-	1000	-	2000	-	1000
River gravel (4-8 mm) (gr)	-	2000	-	-	-	2000	-	-	-
Cement paste composition									
Cement (gr)	351	351	351	351	351	351	298	298	298
Silica fume (gr)	-	-	-	-	-	-	53	53	53
Water (gr)	105	105	105	105	105	105	105	105	105
Superplasticizer (gr)	1.00	1.00	0.97	0.97	0.97	0.97	1.30	1.30	1.30
Set retarder (gr)	-	-	1.20	1.20	1.20	1.20	1.20	1.20	1.20
Compaction	low	low	high	high	high	high	high	high	high

2.2 Test Setup and Instrumentation

The impact tests were carried out using an instrumented drop-weight impact test setup. In the experiment, the specimen was placed vertically on a steel base structure, which also serves as a steel buffer plate that functions as a wave sink at the impact experiments. The impactor was dropped from approximately 1.2 m to provide striking velocities ranging between 4.0 - 4.7 m/sec. The selection of the impactor material and the magnitude of the impact velocity determine the pressure applied to the concrete sample. Therefore, by varying those properties, the input pressure could be controlled. The impactors that were made of either steel or aluminium were 110 mm in diameter and 220 mm in height.

A Doppler laser vibrometer was used to measure the velocity of the falling impactor. For the purpose of measuring the velocity of the interface between the impactor and the target, an easily applicable measurement method has been introduced and verified. The impactor diameter (110 mm) was selected to be larger than the diameter of the target (60 mm) so that there was an outer rim of 25 mm

present to take velocity measurements at the interface. The point where the laser beam hits the impactor was adjusted to be as close as possible to the specimen perimeter, in the inside locations of the rim. The laser beam coming from the laser head following a horizontal path was reflected by an angle of 90° from a 45-degree mirror such that it was directed vertically upwards. The reflected vertical beam hitting the retro-reflective sticker attached to the bottom surface of the impactor rim was then reflecting and following the same path back to the laser head. The captured particle velocity time histories of the interface between the target and the impactor were subsequently processed to determine the impact stress applied on the target. The schematic figure showing the general view of the testing system and an enlarged view of the orientations of the retro-reflective sticker and the 45-degree mirror are presented in Figure 1.

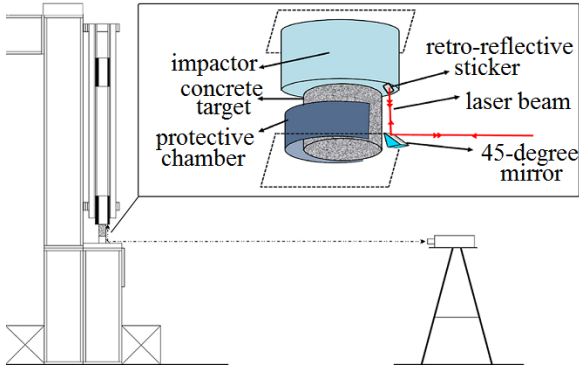


Figure 1: Schematic view of the measurement configuration

During the test, after the free falling impactor hits the stationary target specimen with the impact velocity, it starts to decelerate as expected. After its velocity is decreased due to its contact with the target, the impactor is subsequently brought to rest by a protective chamber, which acts as a stopper (shown in Figure 1). The height of the protective chamber was approximately 2.5 cm shorter than the specimen height. After the collision with the target, the impactor was stopped by the protective chamber to protect the target, which had already failed due to the stress waves, from being fully crushed by self-weight of the impactor. This was done also because the sizes of the broken fragments were critical in evaluating the feasibility of using porous concretes for safety applications. The two impactors used in the tests were made of steel and aluminium. The material properties of the impactors used are critical in the sense that they are directly involved in the impact stress calculations. Using the Young's modulus of elasticity and the Poisson's ratio values provided by the manufacturer, the shear and bulk moduli were calculated. The longitudinal wave velocities of the materials of the impactors were then calculated adopting Eq. 1. The material properties of the impactors are presented in Table 2.

$$C_l = \sqrt{\frac{K + \frac{4}{3}G}{\rho}} = \sqrt{\frac{E(1-\nu)}{\rho(1+\nu)(1-2\nu)}} \quad (1)$$

Table 2: Properties of the materials used in the impactors

Material properties	Steel	Aluminium
Young's modulus of elasticity, E (GPa)	200	69
Density, ρ (g/cm ³)	7.9	2.7
Poisson's ratio, ν	0.28	0.33
Shear modulus, G (GPa)	78.1	25.9
Bulk modulus, K (GPa)	151.5	67.7
Longitudinal wave velocity, C_l (m/sec)	5690	6155

3. MEASUREMENT AND ANALYSIS TECHNIQUES

After the impactor strikes the target specimen, two compression waves propagate away from the interface between the impactor and the target specimen while the interface itself moves downwards with the particle velocity as a result of the shock wave passing over the particles.

3.1. Impedance Mismatch Method

When analyzing shock waves in solids, it is widely accepted to approximate compression paths with the Hugoniot curve. The pressure-particle velocity Hugoniot is the locus of all the possible states that can be achieved when a single shock wave passes through a material at a given initial state [17,18]. In application, the weak shock assumption is usually made, which is valid until shock waves are encountered with very large jumps in stress. The weak shock assumption can be made until a jump in stress around 270 GPa for steel. When the material obeys the weak-shock assumption, the response path of the compression wave is coincident with the Hugoniot [19]. The weak shock assumption is, therefore, valid for the current study where the metal impactors are exposed to much lower stresses.

The shock causes the material to jump between two points on the Hugoniot curve. These points are located at the intersections of the Hugoniot curve and the chord named as the Rayleigh line, connecting the initial state and final shocked state. The slope of this line is equal to the dynamic impedance (Z) of the

material $Z=\pm\rho C$, where ρ and C are the density and the related wave velocity of the material, respectively. Hugoniot with slope discontinuities due to transition from elastic to plastic behavior can thus have regions for which the initial state cannot be connected to the final state with a single Rayleigh line. In such cases the final state is reached by a series of two or more Rayleigh lines. At moderate pressures, Hugoniot of many materials are in their linear range [17-19].

When an impactor strikes a target with an impact velocity, the impact surface between the impactor and the target constitutes a discontinuity in particle velocity. The particle velocity (u_p) is zero inside the target and is equal to the impact velocity (u_i) inside the flyer plate, while the pressure is the ambient atmospheric pressure (P_0). Decomposition of the discontinuity causes the formation of two shock waves that propagate from the impact surface into the impactor and the concrete target, travelling in opposite directions [18]. In most planar impact studies, the pressure versus particle velocity relationship is analyzed using the main features of a method where the Hugoniot curves are intersected, which is called the impedance mismatch method. The graphical presentation of the impedance mismatch method is illustrated in Figure 2. The principle of equal pressures and particle velocities at the interface is satisfied at point $P=P_1$, $u_p=u_1$ which is also the intersection of the two Hugoniot [18].

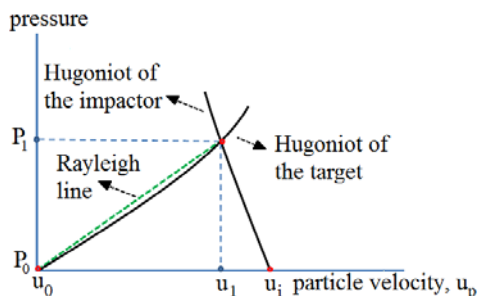


Figure 2: Graphical presentation of the impedance mismatch method

3.2. Reverberation technique

The experimental configuration in the tests performed for this study was slightly different

from the impact situation described above, where there is one interface present. In the tests conducted for this investigation, a low impedance target material, like a porous or normal concrete, is hit by a higher impedance impactor such as steel, while the steel base structure of the setup constitutes a second interface with the target material and causes the compression wave to reflect back into the specimen. Therefore, the situation in these tests can be considered to be a low impedance material that is impacted while being located between two high impedance media.

A one-dimensional stress wave propagating in different media can be presented using a Lagrangian diagram where x is the spatial coordinate and t is time. Even though the interface between the impactor and the target moves downwards with the particle velocity (u_p), this should not be observable in the diagram when compared to the speed of the wave itself [20]. However, because the motion of the interface between the impactor and the target is measured during the experiments, the displacement of the interface is also shown in the diagram given in Figure 3. In the diagram, time $t=0$ corresponds to the instant of collision.

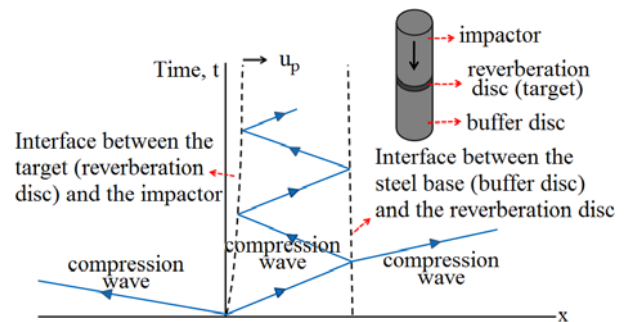


Figure 3: Lagrangian diagram for a low impedance material impacted between two high impedance media

The configuration where the sample is impacted between two materials of higher dynamic impedances has been investigated by several researchers [17,29,22]. In those experiments, a projectile disc (or impactor) is impacted onto a stationary target, which is also called the reverberation disc, made of a linear elastic material having a lower dynamic impedance than the disc that strikes it. The

schematic presentation of the discs is also included in Figure 3. The target is backed by a buffer disc again with a higher dynamic impedance than itself. With the collision, two compression waves propagate away from the interface between the projectile disc and the target. The reflection and transmission of a wave at an interface between two materials depend upon the ratio of their dynamic impedances $K=Z^{MAT I}/Z^{MAT II}$. The reflected wave keeps the sign of the incident wave when the dynamic impedances of the materials from which it reflects are higher than the dynamic impedance of the material it propagates in. Therefore, depending on the relative values of the impedances of the target and the two discs that are in contact with it, each reflection successively increases the amplitude of the compression wave propagating in the target.

Because the target has a much shorter height compared to the thicknesses of the projectile and buffer discs, many wave reflections take place after the collision. In the corresponding reverberation studies presented in literature, the target is a linear elastic material with a dynamic strength that is sufficient to withstand the maximum stress that can be applied by that test configuration at that impact velocity. This maximum stress corresponds to the intersection of the Hugoniot curves of the projectile and buffer disc materials. Therefore, stress continues to increase until that final value is reached through multiple reverberations which is also considered to be a state of equilibrium in pressure [17,29,22]. This situation is illustrated in Figure 4, where the impedance mismatch technique is applied in a special manner because of the repetitive reflections and the presence of two interfaces. Different from the typical impedance mismatch representation illustrated in Figure 2, in Figure 4 the two main inclined lines are the Hugoniots of the impactor and the buffer disc materials, while the lines that travel between those two Hugoniots represent the behavior of the reverberation disc material that is compacted in between. The Hugoniot lines of the impactor and the buffer material intersect

at stress (P_e) and particle velocity (u_e) values that can be considered to be an equilibrium for pressure. The figure also illustrates how the amplitude of a compressive shock wave in the target specimen increases, where the compressive stress is taken positive.

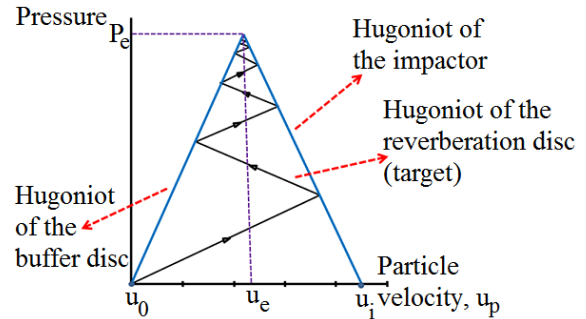


Figure 4: Impedance mismatch graph for a linear elastic reverberation disc

This analysis can also be applied when testing nonlinear materials with dynamic strengths that are not sufficient to withstand the maximum stress that can be applied by the test configuration. In the tests conducted in this research, the targets being either porous concrete or normal concrete, makes the reverberation process slightly different. Similar to the case described above, the target has a small height compared to the impactor and the steel base structure. Therefore, the shock wave that travels in the target again makes some reflections before waves that travel in the impactor and the setup reflect back as tension waves from the top surface of the impactor and the bottom surface of the test setup, respectively. Because of its height, the steel base structure can even be considered as a wave sink. However, different from the reverberation process that occurs when a strong linear elastic material is tested, the reverberation situation in the tests performed for this study continues until the stress within the concrete specimen reaches a value that generates substantial inelastic strains in the material beyond which further wave propagation within the specimen can be neglected. The amplitude of the subsequent wave fronts will be very small [23]. This situation and the related wave reverberations can be seen in the impedance mismatch figure

illustrated in Figure 5. The spots indicated on the Hugoniot of the impactor represent the points where the Hugoniot of the impactor and the target material intersect i.e. the points where the stress and particle velocities of the target and the impactor are equal. In the figure, those points eventually come to an equilibrium level that corresponds to a constant value of stress (P_e).

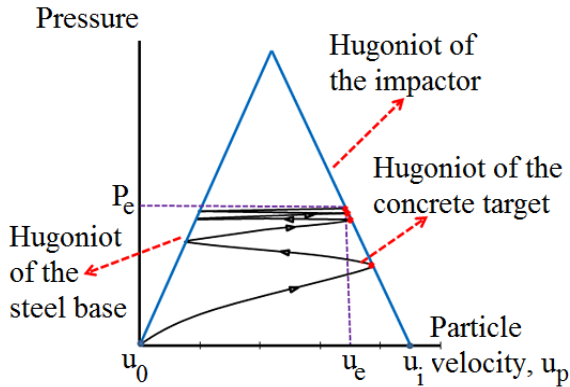


Figure 5: Impedance mismatch graph for a concrete target impacted between two metals

The velocity values of those points are measured by the laser Doppler velocimeter during the test when the falling impactor and the target come into contact and with the subsequent reverberations, the pressure comes to equilibrium.

Because the particle velocity is measured at the interface, on the impactor, it reaches an approximately constant value when the pressure reaches equilibrium, as seen in Figure 5. This velocity value is named equilibrium velocity (u_e).

3.3. Analysis of particle velocity histories

The particle velocity becoming nearly constant as the pressure reaches equilibrium can be seen in the velocity histories measured during the tests. In Figure 6, a typical Doppler laser velocimetry signal from a drop weight impact experiment of porous concrete impacted by a steel impactor is given. In the figure, the first part that seems horizontal corresponds to the free fall of the impactor and has a slope that is very slightly lower than gravitational acceleration, due to the friction between the impactor and the setup. After the

free fall part, there is the collision followed by wave reverberations that end up at the equilibrium of the stress that also corresponds to a nearly constant particle velocity. The plateau corresponding to this equilibrium state is clearly observed in all the tests conducted on porous concretes and the normal concrete using a steel impactor. The last part of the plateau in the figure corresponds to the part, at which the impactor hits the protective chamber (shown in Figure 1) that has a shorter height than the specimen, where the particle velocity very rapidly becomes zero.

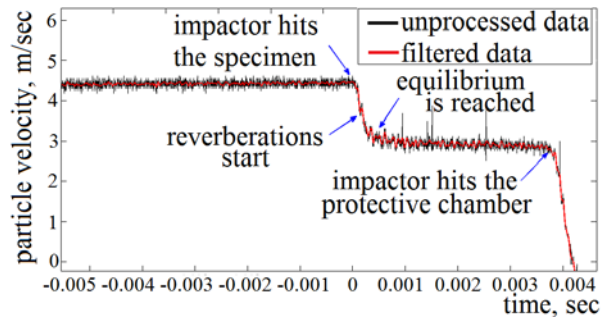


Figure 6: Doppler laser velocimetry signal from a drop weight impact test of porous concrete

Since the particle velocity value that corresponds to equilibrium in pressure, i.e. the equilibrium velocity, is extracted from the very beginning of the plateau, this last portion of the data has no significance. Along with the raw data that is measured with the frequency of 400 kHz, the filtered data with a cutoff frequency of 20 kHz is presented in the figure. In Figure 6, if the time at which the equilibrium velocity is reached after the impact is observed, it can be seen that, this amount is higher than the amounts of time at which the peak forces are reached in the studies of very high speed impact testing in the literature. This is caused by the low impact velocity and therefore the low strain rate of the drop weight impact test performed. In low velocity impact studies, it was presented that the time after impact to reach the peak force decreased as the velocity of the projectile increased. For velocities varying between 26-93 m/sec, the peak force was reached at a time range of 0.05-0.60 msec, respectively [14,24]. Therefore, the time to

reach the equilibrium velocity in the current study is consistent with the results presented in the related studies.

To be able to obtain the stress from the particle velocity measurements, conservation of linear momentum law is used. The conservation law is actually the principle behind the impedance mismatch calculations where the stress is calculated using the equilibrium velocity and the slope of the Hugoniot of the impactor which is the dynamic. According to the conservation equation, the pressure P applied to the target material is determined by the linear momentum transferred by the impactor to the target per unit time as shown in Eq. 2

$$P - P_0 = \rho_0 C(u_i - u_e) \quad (2)$$

where, P , P_0 , ρ_0 , C , u_i and u_e are the shock pressure, initial pressure, initial density, wave velocity, impact velocity and the equilibrium velocity, respectively. For shock waves travelling in solids, the shock pressure P is much greater than the initial pressure P_0 , which is the ambient atmospheric pressure. As the equilibrium in pressure is reached, while the stationary target material with zero velocity reaches an approximately constant particle velocity corresponding to the equilibrium in pressure, the impactor with the impact velocity decelerates down to the same velocity [17]. Therefore, the analyses of the particle velocity histories were done by first extracting the impact and equilibrium velocities from the experimental graph as in Figure 6 and then by using those to determine the stress through impedance mismatch and therefore conservation of linear momentum calculations.

Since the concretes that were tested in the experiments have failed, the stress that is calculated is the dynamic strength of the specimen tested. The key feature of this technique is that the stress is calculated using the dynamic impedance properties of only the impactor and that the properties of the target are not involved in the calculations. Therefore, while all the information is

obtained from the well-defined metal drop weight, the target can be an unknown material.

4. RESULTS AND DISCUSSION

In the tests, the particle velocity histories were measured for a total of nine different types of porous concretes and one mixture of normal concrete.

4.1. Impact test results of porous concretes tested with different impactors

In the first series of results presented, two different types of porous concretes were tested by impacting each type with two different types of impactors (steel and aluminium). The purpose of performing these tests was validating the consistency of the technique by testing the specimens from the same mixture with two different impactors having different dynamic impedances. In the tests, it was proved that the same dynamic strength values are obtained through using different impactors as seen in Table 3.

The averages of the dynamic strength results were 26.26 (with a standard deviation (std) of 2.61 MPa) and 25.48 MPa (std 1.71 MPa) for PRC1 tested with steel and aluminium impactors, respectively. The average results for PRC2 were 21.84 (std 2.22 MPa) and 22.93 MPa (std 1.29 MPa) again for steel and aluminium impactor tests, respectively. The results obtained for the same mixture, when tested with two impactors having different dynamic impedances were consistent for both porous concrete mixtures. This validates that the measurement principle holds irrespective of the type of metal selected for the impactor. From the comparison of the test results obtained with different impactors, it can be said that as the dynamic impedance of the impactor increases, equilibrium velocity is also higher and the difference between impact velocity and the equilibrium velocity is lower.

Table 3: Results of impact tests on porous concretes tested with different impactors

Mixture code	Impactor	Sample no	Impact velocity (u_i) (m/sec)	Particle velocity at pressure equilibrium (u_e) (m/sec)	Δ Particle velocity (m/sec)	(Δu)	Dynamic strength (from Eq. 2) (MPa)
PRC1	steel	1	4.46	3.90	0.56	25.17	
PRC1	steel	2	4.34	3.72	0.62	27.86	
PRC1	steel	3	4.30	3.67	0.63	28.31	
PRC1	steel	4	4.34	3.73	0.61	27.42	
PRC1	steel	5	4.33	3.84	0.49	22.02	
PRC1	aluminium	1	4.58	2.91	1.67	27.75	
PRC1	aluminium	2	4.59	3.08	1.51	25.09	
PRC1	aluminium	3	4.65	3.13	1.52	25.25	
PRC1	aluminium	4	4.52	2.94	1.58	26.24	
PRC1	aluminium	5	4.56	3.17	1.39	23.09	
PRC2	steel	1	4.43	3.95	0.48	21.57	
PRC2	steel	2	4.40	3.88	0.52	23.37	
PRC2	steel	3	4.47	4.02	0.45	20.22	
PRC2	steel	4	4.49	3.94	0.55	24.72	
PRC2	steel	5	4.55	4.12	0.43	19.33	
PRC2	aluminium	1	4.46	3.03	1.43	24.19	
PRC2	aluminium	2	4.49	3.07	1.42	23.56	
PRC2	aluminium	3	4.54	3.28	1.26	20.85	
PRC2	aluminium	4	4.34	2.93	1.41	23.43	
PRC2	aluminium	5	4.41	3.11	1.30	22.63	

Table 4: Results of the impact tests conducted on different types of porous concretes

Mixture code	Impactor	Dynamic strength (calculated using Eq. 2) (MPa)					Porosity (%)	Average dynamic strength (MPa)	Average static compressive strength (MPa)	DIF
PRC1	steel	25.17	27.86	28.31	27.42	22.02	24.75	26.26	15.94	1.60
PRC2	steel	21.57	23.37	20.22	24.72	19.33	-	21.84	13.09	1.73
PRC3	steel	68.76	66.07	67.41	66.97	63.37	21.78	66.52	34.78	1.91
PRC4	steel	73.30	79.59	75.86	76.09	79.05	20.33	76.78	41.89	1.83
PRC5	steel	84.81	80.72	81.21	96.40	86.79	18.77	85.99	50.49	1.70
PRC6	steel	60.63	53.84	60.36	48.27	58.02	17.93	56.22	29.64	1.90
PRC7	steel	55.91	59.64	53.75	45.66	50.47	21.98	53.09	31.60	1.68
PRC8	steel	79.41	81.44	83.28	74.63	-	20.12	79.69	44.81	1.78
PRC9	steel	75.86	90.25	77.93	93.89	83.91	18.63	84.37	48.80	1.73

4.2. Impact test results of different types of porous concretes

According to the results obtained, the aggregate properties and compactive effort are

the main factors that affect the dynamic performance of porous concrete. The results of the porous concrete tests are presented in Table 4. When mixtures containing different

shapes and types of aggregates are compared, it is seen that increased texture and angularity contribute to porous concrete. When two sizes of aggregates were used instead of using single sized aggregates, the dynamic strengths of porous concretes as well as their static strengths increased. This is due to the aggregates having different sizes showing a more efficient packing.

Compaction is a factor that has a very important effect on the strength properties because it directly affects the porosity. As intensive compaction enhances the strength properties, insufficient compaction caused a drastic decrease in both the static and the dynamic strengths. While aggregate properties drastically affect the strength properties, changing the cement paste composition did not have a very significant effect on the dynamic strengths of the samples.

4.3 Impact test results of a moderate strength normal concrete

To be able to verify whether the experimental technique can be used for a moderate strength normal concrete or not, tests were also performed on a normal concrete. As in the impact tests of porous concrete samples, in normal concrete testing, the plateau was very clearly observed and the samples were completely fractured during the test. The results of the tests conducted on the normal concrete are presented in Table 5.

Table 5: Results of the impact tests conducted on normal concrete

Test no	Impact velocity (m/sec)	Equilibrium velocity (m/sec)	Dynamic Strength (from Eq. 2) (MPa)
1	4.29	1.34	60.22
2	4.36	1.29	57.98
3	4.08	1.25	56.18
4	4.38	1.39	62.47
5	4.34	1.23	55.28
6	4.29	1.27	57.08
7	4.35	1.26	56.63

The average of the drop weight impact strength results obtained from the testing of normal concrete was 57.97 MPa while the

average static strength of the samples from the same concrete mixture was 26.44 MPa which corresponds to a dynamic increase factor (ratio of the dynamic material strength to static strength) of 2.19. Dynamic increase factor, DIF, has widely been used as an indication of the effect of strain rate, $\dot{\epsilon}$, on the strength of cementitious materials. The relation between DIF and the strain-rate in concrete was investigated by CEB where DIF formulas for concrete (Eq. 3) were recommended in which a bilinear relation between DIF and $\log \dot{\epsilon}$ with a breakpoint at the strain rate of 30 sec^{-1} was defined [25].

$$DIF = \frac{f_{cd}}{f_{cs}} = \left[\frac{\dot{\epsilon}}{\dot{\epsilon}_s} \right]^{1.026\alpha_s} \quad (\text{for } \dot{\epsilon} \leq 30 \text{ sec}^{-1})$$

and

$$DIF = \gamma_s \left[\frac{\dot{\epsilon}}{\dot{\epsilon}_s} \right]^{1/3} \quad (\text{for } \dot{\epsilon} \geq 30 \text{ sec}^{-1}) \quad (3)$$

where f_{cd} and f_{cs} are the uniaxial dynamic and quasi-static compressive strengths, respectively. In the equations, $\dot{\epsilon}_s = 30 \times 10^{-6} \text{ s}^{-1}$, $\gamma_s = 10^{(6.156\alpha_s - 2.0)}$, $\alpha_s = 1/(5 + 9f_{cs}/f_{co})$, $f_{co} = 10 \text{ MPa}$. At the strain rate of 68 sec^{-1} , the DIF value is calculated to be 2.15 according to Eq. 3 which is very close to the value of 2.19 that was obtained experimentally for normal concrete. The DIF value obtained for normal concrete is also consistent with the widely referenced review on the effect of strain rate conducted by Bischoff and Perry [26]. Recent research led to various models and updates for the CEB formula, while for the moderate strength increase regime, the overall order of magnitude is still valid [27].

4. CONCLUSIONS

In the research presented in this study, the experimental configuration that has been developed for the determination of the dynamic response of porous concretes in a drop weight impact test was described. The results of the drop weight impact tests conducted on different types of porous concretes and a moderate strength normal concrete were also presented. The main features of the work can be summarized as follows:

-The motion of the interface, i.e. the particle velocity at the interface between the impactor and the concrete specimen, could be monitored accurately by using the experimental configuration introduced. Laser Doppler Velocimetry technique was used for monitoring the particle velocity at the interface.

- The velocity measurements were analyzed using a special reverberation application of the impedance mismatch method.

- The measurement technique was proven to be consistent by testing the same type of porous concrete specimens using both steel and aluminium impactors. Although the dynamic impedance of the impactor was varied, the same stress results were obtained.

- The testing technique was applied on porous concretes having different dynamic strengths and was proven to be sufficient in testing porous concrete. It was also validated that the measurement technique could be used on normal concrete as well, provided that a high dynamic impedance impactor such as steel is used in testing.

- The testing configuration can be used to test a large number of samples in a short time and it is a non-contact monitoring method where no sensors are installed.

- The experimental configuration and the subsequent analysis technique also has the advantage of involving only the well known dynamic impedance properties and the velocity measurements of the impactor, while the target specimen that is tested is not directly involved in the measurements or the analysis.

- According to the porous concrete test results obtained, the aggregate properties, such as grading, size, shape, texture and strength, and compactive effort are the main factors that affect the dynamic performance of porous concrete while cement paste properties were not as effective.

ACKNOWLEDGEMENT

This project was funded by the Netherlands Ministry of Defence. We would also like to acknowledge the Engineering Dynamics Section of the Faculty of Mechanical,

Materials and Maritime Engineering at Delft University of Technology for providing the laser Doppler velocimetry equipment. We would also like to thank Ger Nagtegaal and Gerard Timmers for their contributions to establishing the test setup.

REFERENCES

- [1] Yang J, Jiang G., 2003. Experimental study on properties of pervious concrete. *Cem. Concr. Res.* **33(3)**:381–386.
- [2] Chindaprasirt P, Hatanaka S, Chareerat T, Mishima N and Yuasa Y., 2008. Cement paste characteristics and porous concrete properties. *Constr. Build. Mat.* **22(5)**:894-901.
- [3] Ghafoori N, Dutta S., 1995. Development of no-fines concrete pavement applications. *J. Trans. Eng.* **121(3)**: 283-288.
- [4] Marolf A, Neithalath N, Sell E, Wegner K, Weiss J, Olek J., 2004. Influence of aggregate size and gradation on the acoustic absorption of enhanced porosity concrete. *ACI Mat. J.* **101(1)**: 82-91.
- [5] Espinosa, H. D., 2000. *Low-velocity impact testing*. ASM handbook.
- [6] Grady, D. E., 1996. *Shock equation of state properties of concrete*. Sandia National Labs.
- [7] Reinhart, W. D., Chhabildas, L. C., Kipp, M. E. and Wilson, L. T., 1999. Spall strength measurements of concrete for varying aggregate sizes. *Proc. of 15th US Army Symposium on Solid Mechanics*, April 12-14, 1999, Myrtle Beach, South Carolina, USA. pp. 1-14.
- [8] Chhabildas, L. C., Grady, D. E., Hall, C. A. and Reinhart, W. D., 2002. *Dynamic properties of concrete through particle velocity profile measurements*. Sandia National Labs.

- [9] Gustavsen, R. L., Sheffield, S. A., Alcon, R. R. and Hill, L. G., 1999. *Shock initiation of new and aged pbx 9501 measured with embedded electromagnetic particle velocity gauges*. Los Alamos National Laboratory.
- [10] Rosenberg, Z., Meybar, Y. and Yaziv, D., 1981. Measurement of the Hugoniot curve of Ti-6Al-4V with commercial manganin gauges. *J of Phys D: Appl. Phys.* **4**: 261-266.
- [11] Sukontasukkul, P., Nimityongskul, P. and Mindess, S., 2004. Effect of loading rate on damage of concrete. *Cem. Concr. Res.* **34**: 2127-2134.
- [12] Unosson, M. and Nilsson, L., 2006. Projectile penetration and perforation of high performance concrete: experimental results and macroscopic modelling. *Int. J Imp. Eng.* **32**: 1068-1085.
- [13] Yeh Y, Cummins H.Z., 1964. Localized fluid flow measurements with an He-Ne laser spectrometer. *Appl. Phys. Let.* **4(1)**:176-178
- [14] Wu, E., Sheen, H. J., Chen, Y. C., Chang, L. C., 1994. Penetration force measurement of thin plates by laser Doppler anemometry. *Exp. Mech.* **34**: 93-99.
- [15] Birch, R.S. and Jones, N., 1990. Measurement of impact loads using a laser Doppler velocimeter. *Proc. of the Inst. of Mech Eng. Part C, J Mech. Eng. Sci.* **204**: 1-8.
- [16] Hodgkinson, J. M., Vlachos, N. S., Whitelaw, J. H. and Williams, J. G., 1982. Drop-weight impact tests with the use of laser-Doppler velocimetry. *Proc.R. Soc Lond.*, **379**:133-144.
- [17] Kanel, G. I., Razorenov, S. V. and Fortov, V. E., 2004. *Shock-wave phenomena and the properties of condensed matter*. Springer-Verlag.
- [18] Meyers, M. A., 1994. *Dynamic behavior of materials*. John Wiley & Sons.
- [19] Drumheller, D. S., 1998. *Introduction to wave propagation in nonlinear fluids and solids*. Cambridge University Pres.
- [20] Zukas, J. A., 1990. *High velocity impact dynamics*. John Wiley & Sons.
- [21] Lysne, P.C., Boarde, R.R., Percival, C.M., and Jones, O.E., 1969. Determination of release adiabats and recented Hugoniot curves by shock reverberation techniques. *J. Appl. Phys.*, **40**:3786-3795
- [22] Kondo, K., Yasumoto, Y., Sugiura, H., Sawaoka, A., 1981. A multiple shock reverberations in a layer structure observed by particle velocity and pressure gauges. *J. Appl. Phys.*, **52**: 772-776.
- [23] Ramesh, K. T., 2009. *High strain rate and impact experiments-Handbook of experimental solid mechanics*, Springer.
- [24] Perez-Castellanos, J. L., Cortes, R., Fernandez-Saez, J. and Navarro, C., 1997. Numerical simulation of the impact of projectiles on thin aluminium plates. *J. Phys. IV France*, **7**: 711-716.
- [25] Comité Euro-International du Béton, 1993. *CEB-FIP Model Code 1990*, Redwood Books.
- [26] Bischoff P. H., Perry S. H., 1991. Compressive behaviour of concrete at high strain rates. *Mat.Struct.*, **24(6)**:425-450.
- [27] Weerheijm J., Vegt I. and Breugel van K., 2009. The rate dependency of concrete in tension – New data for wet, normal and dry conditions. *Proc. DYMAT*, September 7-11, 2009, Brussels, Belgium; pp.95-101.